Planet. Space Sci., Vol. 30, No. 2, pp. 151–167, 1982
Printed in Great Britain.

0032–0633/82/020151–17$03.00/0

A NEW LOOK AT THE IONOSPHERE OF JUPITER IN LIGHT OF THE UVS OCCULTATION RESULTS

J. C. McCONNELL
CRESS and Physics Department, York University, Downsview, Ontario, Canada, M3J 1P3

and

J. B. HOLBERG, G. R. SMITH, B. R. SANDEL, D. E. SHEMANSKY and A. L. BROADFOOT
Earth and Space Sciences Institute, University of Southern California, Tucson Laboratories, Tucson, AZ 85713, U.S.A.

(*Received* 1 *September* 1981)

Abstract—Simple photochemical models cannot reconcile Jupiter's ionospheric electron density profiles with the observed neutral atmosphere. The location of the peak electron density predicted when the neutral atmosphere determined by the *Voyager* Ultraviolet Spectrometer is combined with simple models falls about 1000 km lower than the peak determined by radio occultation. The locations and magnitudes of the peaks in electron density can be accounted for by including the effects of vertical transport of ions in the ionospheric models. This vertical transport may be induced by meridional winds in the neutral atmosphere or external electric fields. It is probable that precipitating particles and an altitude-variable H_2 vibrational temperature play important roles in determining the character of the ionosphere. In view of the complex relationship between the ionosphere and neutral atmosphere, an attempt to infer one from the other cannot succeed. However, combining independent information on the two leads to new insights into the coupling of the neutral atmosphere, the ionosphere and the magnetosphere.

1. INTRODUCTION

An ionosphere is formed in a planetary atmosphere when energetic photons and particles ionize the neutral gas to create ions and electrons. If the time constants for recombination are long enough then the plasma may diffuse or flow under the influence of electric fields from the region of creation. Analysis of the distribution of such a plasma with height can yield information on the neutral atmosphere and the various physical processes that take place. However, because of the complexity of processes that may occur, unravelling such a distribution can turn out to be a non-trivial process. The more information that is available, the more successful the venture is likely to be.

Electron density profiles for Jupiter's upper atmosphere have been obtained by the *Pioneer* 10 and 11 (P10 and P11) and *Voyager* 1 and 2 (V1 and V2) flybys. These profiles have been analyzed by Atreya and Donahue (1976) and Atreya *et al.* (1979b), using ionospheric models, to yield information on the temperature and neutral density of the Jovian thermosphere. Since their analysis, information has become available on the neutral structure of the thermosphere. Thus we approach the problem from the opposite direction. Instead of inferring the neutral atmosphere from the ionospheric profiles, we use models of neutral density as a basis for calculating electron density profiles. For simple photochemical steady state models we find a serious disparity with the measurements in terms of the altitude and the density of the peak of the electron density profiles. Thus we vary other parameters available to us, such as drift velocity and rate coefficients in an attempt to explain the *Pioneer* and *Voyager* electron density profiles obtained by the radio science experiments. To date, there have been no model calculations applicable to Jupiter that include the vertical drift velocity induced either by electric fields or neutral winds. However, in writing this paper it came to our notice that Strobel and Atreya (1981) had mentioned that the altitude of the Jovian electron density peak could be moved due to the influence of winds.

The information on the neutral density has come from observations of solar and stellar occultations by the *Voyager* Ultraviolet Spectrometers (UVS). The V1 UVS measured the atmospheric absorption of the solar spectrum in the wavelength region 500–1700 Å as the sun was occulted by the atmosphere of Jupiter. The atmospheric occul-

tation of the star α-Leo was also measured by the UVS on V2. Analysis of these data yields information on the temperature and composition of the thermosphere.

We first discuss the ionospheric data from the *Pioneer* and *Voyager* radio science experiments. We next outline the simplified ionospheric model used for comparison and discuss the parameters required, such as neutral atmosphere, reaction rates, solar fluxes and cross-sections and diffusion coefficients. In the next section we also present some model results to aid in a comparison of the theoretical and experimental electron density profiles. Using the model results, we discuss the *Pioneer* and *Voyager* radio science measurements pointing out areas of agreement and disagreement. Finally we present our conclusions regarding the status of our understanding of the Jovian ionosphere.

2. RADIO OCCULTATION RESULTS

The first data pertaining directly to the Jovian ionosphere was obtained when *Pioneer* 10 passed behind Jupiter on 4 December 1973. Data were obtained from both the entrance and exit occultations of the spacecraft radio signal. The entrance occultation was at a latitude of 28° N and during early evening while the exit occultation was at a pre-dawn latitude of 60° N. The occultation experiment used the *S*-band (2.3 GHz) radio-tracking link to probe the atmosphere and ionosphere as the spacecraft–earth link was occulted by the planet. The experiment utilized an on-board crystal oscillator as a frequency reference. At and before the time of occultation this frequency drifted due to the harsh radiation environment. The doppler frequency perturbations imposed on the radio-tracking link were used to study the vertical electron density distribution throughout the probed regions. Figure 1(a), curve A, shows the electron density calculated assuming a continuous drift of the oscillator (Fjeldbo *et al.*, 1975). The relevant parameters are given in Table 1. The topside plasma scale height for the entrance is about 975 km, while for exit it is about 800 km. Also noted in Fig. 1(a) are some of the principal layers, L_i, identified by the *Pioneer* radio science investigators. Many of these features, especially the lower ones, may be artifacts of the inversion process due to problems with multipath propagation and ionospheric inhomogeneities that cannot adequately be allowed for. A distinct feature on both entrance and exit is the L_1 peak at around 1600 km,* even though it is less pronounced on the morningside. The L_2 ledge occurs about 1100 km, while the L_3 peak is at 900 km on the morningside and about 800 km on the eveningside. Curve A′ in Fig. 1(a) shows the result of an analysis of the occultation data assuming different conditions for the oscillator drift rate. Although the change in the plasma scale height (from 975 to 375 km) and electron density (9×10^4 to 3×10^4 at the L_1 ledge) are considerable certain features remain, namely the L_1, L_2 and L_3 peaks and ledges.

For the P11 flyby on 3 December 1974, the experiment was improved by transmitting to the spacecraft an earth-based stable reference

*All heights in this report are referenced to the 1 mb level.

TABLE 1. SUMMARY OF IONOSPHERIC OCCULTATIONS

	Pioneer				*Voyager*			
	10		11		1		2	
	En†	Ex‡	En	Ex	En	Ex	En	Ex
Date	4 Dec. 73		3 Dec. 74		5 March 79		9 July 79	
Latitude	26°N	58°N	79°S	20°N	12°S	1°N	67°S	50°S
Longitude	45°W	260°W	263°	61°W	63°W	314°W	255°W	148°W
S.Z.A.	81°	95°	93°	79°	82°	98°	88°	92°
Dip angle I	−27.3	−51.9	+87.7	−8.2	+45.4	−16.1	−53.0	−85.5
Time of day	evening	predawn	morning	a'noon	a'noon	predawn	evening	dawn
H_p(km)	675 ± 300	800	540 ± 60	?	590,960	960	1040	880
T*(K)	900 ± 400	1160	850 ± 100	?	760,1150	1190	1600	1200
L_1 height (m)	1600	1500–1900	1500	1800	1600	2300	< 600	1900
L_3 height(km)	800	900	1000	750	?	?	?	?
$N_e(l_1)$	3.4–8.5(4)	≅ 1.5(4)	4(4)	?	2.2(5)	1.8(4)	> 2(5)	2(5)
$N_e(L_3)$	1–2(5)	3.5(5)	1.8(5)	?	?	?	?	?

*T is calculated from H_p assuming that the scale height reflects H^+ in diffusive equilibrium and $T_i = T_e = T$.
†En = entrance; ‡Ex = exit.

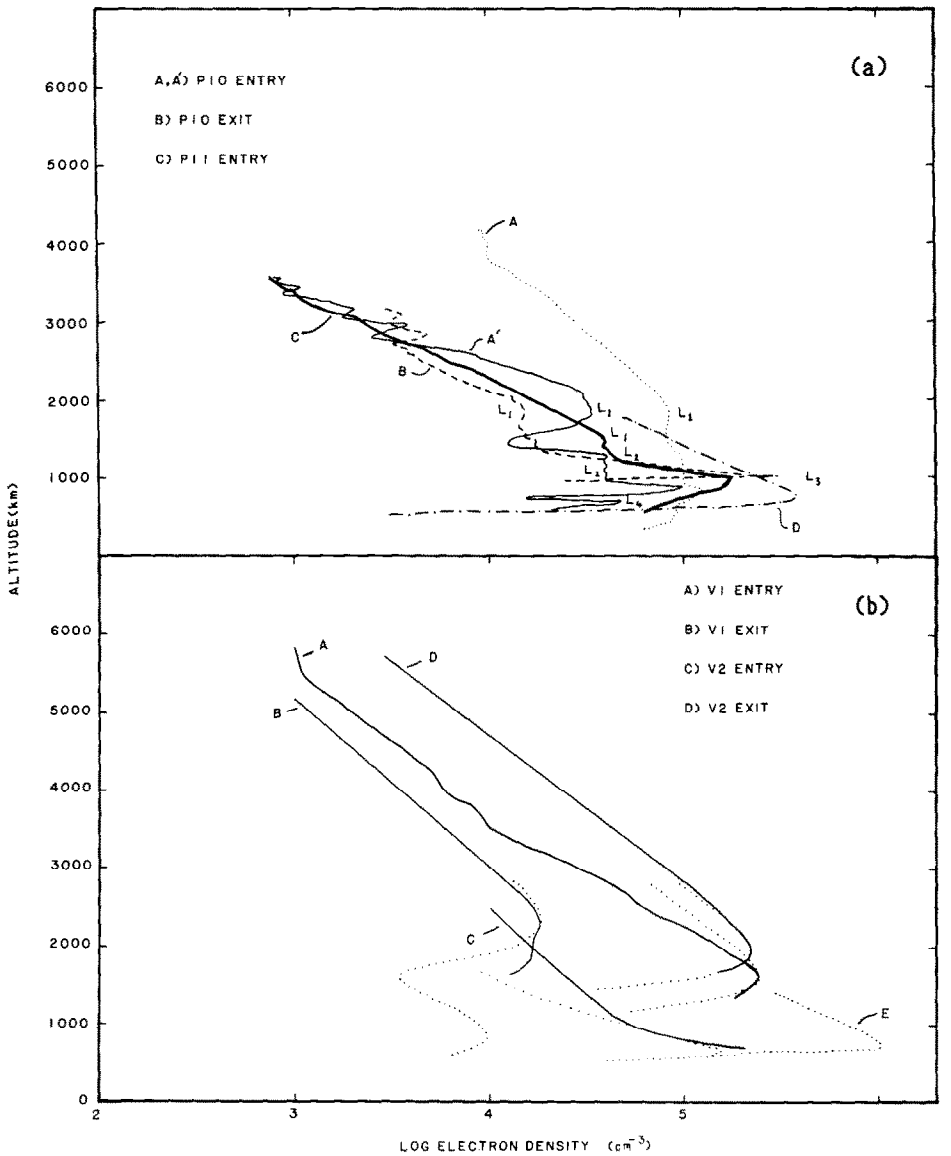

FIG. 1(a). SKETCH OF PIONEER ELECTRON DENSITY PROFILES VS ALTITUDE.
Curve A and A' are derived from the same data set. A: P10 entry; B: P10 exit; C: P11 entry. For details see Table 1. Curve D is a model electron density profile obtained using model atmosphere A (see Fig. 2) with H reduced by 100 and solar fluxes reduced by 3 to simulate Pioneer.

FIG. 1(b). SKETCH OF VOYAGER ELECTRON DENSITY PROFILES.
A: V1 entry; B: V1 exit; C: V2 entry; D: V2 exit. Curve E is a model ionosphere calculated using the parameters discussed in the text and with $k_2 = 0$, $W_D = 0$. The dotted curves have been fitted using the parameters discussed in the text. Latitudes, dip angles etc. used are appropriate for the observations and are given in Table 1. Ionization rates were diurnally averaged.

frequency at 2.1 GHz. During entrance this reference frequency was used to generate the 2.3 GHz signal transmitted back to earth and through the Jovian ionosphere from *Pioneer* 11. Thus the entrance experiment did not suffer the same uncertainty as did that of P10. However, as the earth-based uplink signal was lost during immersion, the on-board oscillator was used for exit and the exit information therefore suffers from discontinuous shifts in oscillator frequency due to

radiation effects. Figure 1(a) shows the P11 entrance data for a latitude of 79° S. The topside plasma scale height was 540 ± 60 km. As for P10, the evidence of layers is apparent with the L_1 peak occurring at 1500 km while the L_2 ledge and L_3 peak occur at 1200 and 1000 km. There is a region of smooth change between the L_2 ledge and the L_3 peak. The scale height associated with this region is $\simeq$ 135 km. The exit measurements are much more uncertain and Fjeldbo *et al.* (1976) quote only the altitude of the L_1 and L_3 layers as 1800 and 750 km.

The *Voyager* radio science experiment (RSS) employs improvements over the *Pioneer* experiment, viz. two coherent radio frequencies at 2.3 and 8.3 GHz, increased signal strengths and a radiation-resistant oscillator of improved stability as an on-board frequency reference.

Voyager 1 encountered Jupiter on 5 March 1979. The electron densities derived from the RSS experiment are shown in Fig. 1(b) (Eshleman *et al.*, 1979a). The profiles presented by Eshleman *et al.* (1979a) do not extend much below the first peak which, using the *Pioneer* terminology, we call the L_1 peak. The plasma scale heights measured are 960 km for both entrance and exit on the topside. The entrance profile also has an extensive region below 3500 km to which a scale height of 590 km may be assigned. Both profiles were measured in equatorial regions. The height of the L_1 peak is about 1600 km for entrance and 2300 km for exit. There are also large differences in the dawn to dusk electron densities (1.8×10^4–2.2×10^5 cm^{-3}).

The *Voyager* 2 radio occultation probed Jupiter's atmosphere at more polar latitudes on 9 July 1979. The electron density profiles deduced from the radio occultation data are shown in Fig. 1(b). The preliminary results of Eshlemann *et al.* (1979b) show no evidence of a peak above 700 km on entrance. Thus there is no L_1 peak, the L_2 ledge is not apparent and the L_3 peak must be below 700 km. The plasma scale height is about 1040 km above the 1000 km altitude level and $\simeq$ 240 km below. The exit results place the L_1 peak at 2000 km with an electron density of $\simeq 2 \times 10^5$ cm^{-3}. The plasma scale height is about 880 km over a very extensive region.

What are the main features of the *Pioneer* and *Voyager* results? Except for the P10 entrance occultation (curve A) the *Voyager* topside plasma scale heights are larger than those measured by the *Pioneer* RSS mission. The P10 profiles exhibit an evening to morning decrease in the region of the L_1 peak. However the latitudes at which the measurements were taken are very different. The V1 entrance and exit profiles also suggest an evening to morning decrease for equatorial latitudes. The V2 data are quite different. There is a difference of only 17° in the latitudes of the two V2 profiles. However the entrance profile is in the region of the Jovian auroral oval where heating by precipitating particles is expected to be strong and this may have some bearing on the difference between the entrance and exit profiles. An important similarity between the *Voyager* and *Pioneer* measurements is the occurrence of the L_1 peak around 1700–2000 km. In addition, although absolute densities are uncertain, the *Pioneer* results seem to indicate that the L_3 layer is real and not just an artifact of the data analysis. However, perhaps the most insistent feature of the measurements is their variability; it seems clear that there is no simple trend with latitude or from morning to evening.

There have been many changes in the physical parameters that affect the Jovian ionosphere from the time of the *Pioneer* to *Voyager* encounter. The Jovian disk Lyman α intensity has increased more than twenty-fold indicating an increase in H in the upper atmosphere (Broadfoot *et al.*, 1979; Cochran and Barker, 1979; Sandel *et al.*, 1979; Yung and Strobel, 1980). Helium 584Å intensities indicate a decrease in the mixing in the upper atmosphere (McConnell *et al.*, 1980a). The spectral quality of the ion and neutral tori have also changed dramatically (Judge *et al.*, 1976; Shemansky, 1980). This may be of consequence since the torus may feed ions and energy into the Jovian auroral regions and magnetosphere (Thorne and Tsurutani, 1979; Hunten and Dessler, 1977). In addition, there have been changes in solar activity. The EUV solar flux has increased by a factor of 3 or more (Hinteregger, private communication) in the five years between *Pioneer* and *Voyger* encounters. We will attempt to consider these changes when comparing model calculations with the experimental results.

3. THE IONOSPHERIC MODEL

Much effort has gone into the modelling of the ionospheres of the outer planets with a view to planning the *Pioneer* and *Voyager* missions. However, the level of sophistication of these models is much less than that of models used for the earth since the necessary data base, such as neutral winds, electric fields etc., is not available. Excellent reviews of the subject of ionospheric modelling for the major planets are given by Hunten (1969), McElroy (1973), Atreya and Donahue

(1976), and most recently by Strobel (1979). Huntrees (1974) has reviewed details of ionospheric chemistry. In the upper ionosphere reactions involving the major constituents H_2, H and He are important, while in the lower ionosphere reactions involving the minor constituents such as CH_4, C_2H_2 etc. become important. We are most concerned with the upper ionosphere, thus only reactions involving H_2, H and He are involved. Further, since He does not play a *major* role, due to its low density, and we are concerned with illustrative calculations, we have chosen to ignore reactions involving He. This should cause no change in our discussion. The reactions we have utilized are given in Table 2. We have not included the reaction of H^+ with H_2 via radiative recombination:

$$H^+ + H_2 \rightarrow H_3^+ + h\nu.$$

This reaction appears to have first been suggested by Dalgarno (see Hunten, 1969) and its effects have been investigated by Prasad and Capone (1971) using a steady state model and by Tanaka and Hirao (1973) using a time dependent model. However, Huntress (1974) suggests that the rate should be $< 10^{-19}\,cm^3\,s^{-1}$ making it unimportant in the present situation.

The reaction of H^+ with H_2, k_2,

$$H^+ + H_2 \rightarrow H_2^+ + H \qquad -1.83\,eV$$

is endothermic unless the H_2 is in the fourth or higher vibrational level or unless the H^+ (or H_2) is kinetically hot. McElroy (1973) was the first to point out that much of the photon energy deposited in H_2 may end up in vibrational modes of H_2. He noted that vibrational temperatures could be as high as 700 K, depending on the efficiency of processes that quench vibrationally hot H_2. His calculations included the effect of the diffusion of the vibrationally excited H_2. The solar fluxes used in his calculations were representative of solar minimum conditions. Thus for solar maximum conditions one might expect even higher vibrational temperatures. In addition, the dayside intensities of H_2 Lyman and Werner bands on Jupiter (Broadfoot *et al.*, 1981) indicate an influx of energy in precipitating electrons $\simeq 0.3\,erg\,cm^{-2}\,s^{-1}$. If a substantial fraction of this energy should end up in vibrational excitation via ion–molecule processes and direct excitation

$$e + H_2(v=0) \rightarrow H_2(v>0) + e$$

then we may have vibrational temperatures even higher than those mentioned above. Atreya *et al.* (1979b) and Strobel (1979) have already suggested vibrational excitation of H_2 to account for the day to night variation of the V1 electron density results. We have not attempted to calculate vibrational temperatures; instead we will use the value of k_2 as an adjustable parameter.

The source for the photoionization and absorption cross-sections are given in Table 1. There is some uncertainty in the efficiency of producing H^+ from H_2. The results of Monahan *et al.* (1974) are a factor of 3 less than those of Browning and Fryar (1973) at 584Å. We have chosen the results of Browning and Fryar (1973) and Fryar and

TABLE 2. IONOSPHERIC REACTIONS CONSIDERED

Photoionization		
1. (a)*	$H_2 + h\nu \rightarrow H_2^+ + e$	
(b)	$\rightarrow H^+ + H + e$	
2.†	$H + h\nu \rightarrow H^+ + e$	
3. (a)‡	$H_2 + e \rightarrow H_2^+ + 2e$	
(b)	$\rightarrow H^+ + H + 2e$	
4.	$H + e \rightarrow H^+ + 2e$	
Ion interchange reactions		
1.§	$H^+ + H_2 + M \rightarrow H_3^+ + M$	$3.2(-29)$
2.	$H^+ + H_2 \rightarrow H_2^+ + H$	see text
3.§	$H_2^+ + H \rightarrow H_2 + H^+$	$1.0(-10)$
4.§	$H_2^+ + H_2 \rightarrow H_3^+ + H$	$2.0(-9)$
Ion recombination reactions		
5.‖	$H^+ + e \rightarrow H + h\nu$	$4.35(-12)(33/T)^{0.65}$
6.¶	$H_2^+ + e \rightarrow H + H$	2.0×10^{-8}
7.**	$H_3^+ + e \rightarrow H_2 + H$	$2.3(-7)(300/T)^{0.5}$
	$\rightarrow 3H$	

*Absorption cross-sections, 180–780 Å, Lee *et al.* (1976); 780–840Å, Dalgarno and Allison (1969); $\lambda < 180$Å, Samson (1966) $\lambda > 840$ cross-section set equal to 0. For photoionization efficiency see Hudson (1971), and for dissociative ionization yields see Browning and Fryar (1973) and Fryar and Browing (1973). For $\lambda < 300$Å, we assumed the efficiency of H^+ production rose to 0.12 (cf. Samson, 1972).

†Samson (1966).

‡It was assumed that the photoelectrons produced by photoionization in 1 and 2 caused an additional amount of ionization given by $[(h\nu - IP)/35]$ where IP is the ionization potential of H_2 or H.

§cf. Atreya and Donahue (1976).

‖Bates and Dalgarno (1962).

¶Bardsley and Biondi (1970) quote theoretical calculations yielding values between 3×10^{-8} and 3×10^{-9} at 300K. Measurements of $e + H_2^+$ cross-sections by Auerbach *et al.* (1977) suggest values $> 10^{-8}$ at 300 K. However our results are insensitive to this rate.

**Leu *et al.* (1973).

Browning (1973) because they took care to avoid any mass discrimination effects in their mass spectrometer. In addition, their results for dissociative photoionization of O_2 are in agreement with other workers (cf. Fryar and Browning, 1973). Further, their results at 304Å are in reasonable agreement with an estimate made by Samson (1972). The numbers that we use seem somewhat higher than those of Atreya and Donahue (1976). We believe our numbers are more appropriate for the above reasons. Since H^+ is, in general, the major ion, electron densities are quite sensitive to the yield of H^+ from H_2.

Most of the solar flux that yields H^+ from H_2 is around 200–350Å and so is quite energetic. The protons that are produced have a kinetic energy of around 8 eV (Huntress, 1974) and any endothermicity in reaction k_2 may be readily overcome. However, the cross-section for k_2 at 8 eV is only 0.1 of the total cross-section of H^+ with H_2 at that energy. Also H^+ has a very high rate with H due to symmetric resonance charge transfer. Thus collisions of H^+ with H and H_2 will tend to equilibrate the H^+. For this reason we have chosen not to take into account the effect of hot H^+ from H_2. More detailed calculations might attempt this. The net effect would appear as a slight reduction in the efficiency of H^+ production from photoionization of H_2 at short wavelengths.

The solar fluxes adopted were taken from Atmosphere Explorer data for the time of the *Voyager* 1 encounter (Hinteregger, private communication). Compared to the uncertainty in other parameters of interest, the uncertainty in the intensity of the relevant solar fluxes at the time of encounter is small. Thus we have not varied them. The ionization rates were calculated for a specific latitude and in general were averaged over a Jovian day and the program was run to a steady state. Some runs, however, were run to a cyclic state by allowing the sun to rise and set.

The basis for the neutral atmosphere is the analysis of the V1 U.V. spectrometer solar and V2 stellar occultation measurements. Figure 2 shows two model atmospheres referenced to the 10^8 density level (see below) which produce adequate fits to the solar occultation data. Model A has a base temperature of 200 K, while the base temperature for model B is 400 K. The exospheric temperature for both is 1000 K. However, at the $\tau \simeq 1$ level for H_2 at ~ 700Å in the slant direction the temperature is $\simeq 890$ K. This temperature is somewhat lower than those in the preliminary analysis of Atreya *et al.* (1979a). The current analysis involves a detailed treatment of spacecraft motion and instrumental light scattering characteristics. The details of the analysis will be published at a later date (G. R. Smith, private communication). The more detailed analysis will involve an error analysis of the occultation results.

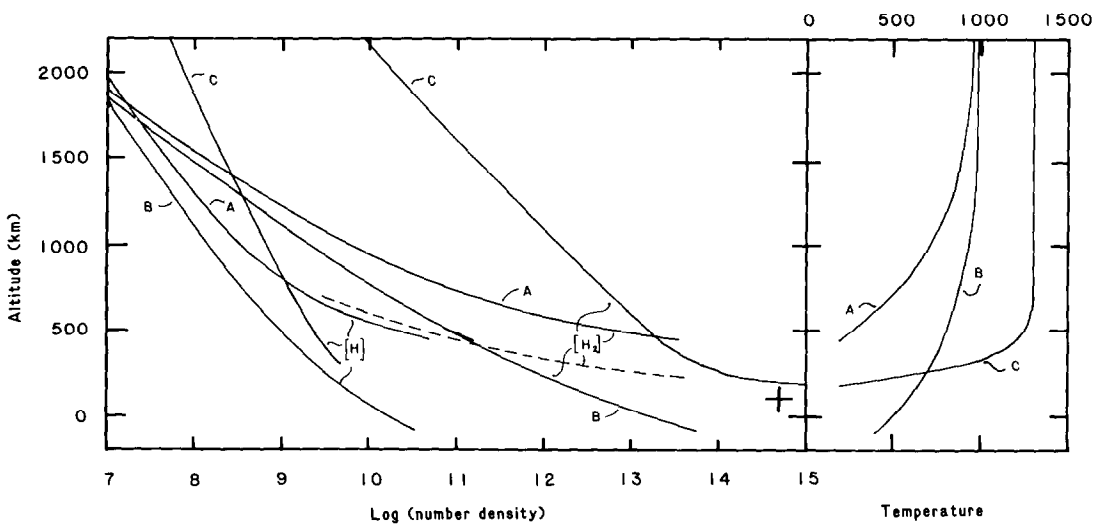

FIG. 2. MODEL ATMOSPHERE DENSITIES AND TEMPERATURES USED IN THE CALCULATIONS. Curves A and B refer to the results of fitting the solar occultation data. Curve C was obtained by adjusting the atmosphere until a reasonable ionospheric profile was obtained. The dashed line represents the stellar occultation results of Festou *et al.* (1981). The + datum is based on the review of Hunten and Veverka (1976).

However, this should not affect the results in the region of concern in this work.

The full size of the sun in the atmosphere was $\simeq 800$ km while the scale height of constituents in the lower atmosphere is $\simeq 50$ km. Thus the altitude uncertainty could be quite large. However, the spectral information available allows us to reduce this uncertainty to that shown in Fig. 2. Further refinement in fitting may reduce this spread. At the top of the atmosphere the scale height of H_2 is $\simeq 150$ km, while that of H is $\simeq 300$ km. The UVS slit is only half filled by the sun. However, the limit cycle motion of the spacecraft, and the spectral information available allow us to locate the 10^8 cm^{-3} density level to better than ± 150 km. Thus from the solar occultation data alone the 10^8 density level is at 1470 ± 150 km while the 10^{11} density level is located at 600 ± 200 km. The results of an analysis of the α-Leo stellar occultation (Festou *et al.*, 1981) are also shown in Fig. 2. Again the 10^{11} density level is found to be within the 400 km uncertainty spread. The significance of the 10^{11} cm^{-3} density level is that here $\tau \simeq 1$ in the vertical for H_2 so for simple photochemical reactions this level should roughly coincide with the location of the ionospheric peak. Also shown in Fig. 2 is a summary of the ground-based stellar occultation results reviewed by Hunten and Veverka (1976). On comparing the results of UVS solar, UVS stellar and ground-based stellar results, it would seem that the density and temperature structure of the lower thermosphere is defined adequately for our purposes.

The atomic hydrogen densities have been taken from the solar occultation results. The vertical column densities of H are compatible with calculations of the solar Lyman α albedo (McConnell *et al.*, 1980a, b) in the region of the atomic H bulge (Sandel *et al.*, 1979). This seems reasonable since the solar occultation occurred in the bulge region. We have also run models with the atomic H abundance reduced by a factor of 100 for comparison with the P11 data (Carlson and Judge, 1974).

We have included diffusion of ions in the background gas, H_2 and H. The ion-neutral diffusion coefficients D_{in} were calculated using the data and formulae given in Banks and Kockarts (1973). The equations to be solved were the continuity equation for each of the ions, H^+, H_2^+, H_3^+,

$$\frac{\partial n_i}{\partial t} + \frac{\partial \phi_i}{\partial z} = P_i - L_i$$

and the flux for each ion was assumed to be given by

$$\phi_i = - D_{in} \sin^2 I \left\{ \frac{\partial n_i}{\partial z} + \frac{n_i}{H_i} + \frac{n_i}{n_e} \cdot \frac{T_e}{T_i} \cdot \frac{\partial n_e}{\partial z} + \frac{n_i}{T_i} \cdot \frac{\partial}{\partial z}(T_e + T_i) \right\} + n_i W_D$$

(Banks and Kockarts, 1973). The vertical drift velocity, W_D, is given by

$$W_D = - aE_y \cos I - bU_n \cos I - V_n \sin I \cos I + W_n \sin^2 I.$$

In the expression for ϕ_i we have neglected the acceleration term. T_e and T_i are the electron and ion temperature respectively, n_i and n_e are ion and electron densities, H_i is the ion scale height and I is the magnetic dip angle. We assumed charge neutrality, i.e. $n_e = \Sigma n_i$. U_n, V_n and W_n are the eastward, northward (meridional) and vertical winds of the neutral atmosphere defined with respect to the plane of the magnetic field. The terms involving a and b are defined by Banks and Kockarts (1973). In the region of interest $b \ll 1$. E_y is the eastward electric field component. Since vertical neutral winds are generally small compared to zonal and meridional winds, the drift velocity mainly arises due to electric fields and meridional winds. In most of the calculations the dip angle for a given geographic latitude was calculated using a simple dipole model aligned with the rotation axis. For a comparison with the *Voyager* data the dip angles listed in Table 1 were used. The bottom boundary was located at about 1.6×10^{12} cm^{-3}. Generally this is sufficiently low so that photochemical steady state (PCSS) was a good approximation. The upper boundary conditions were those suggested by Strobel and McElroy (1970), but we have also done calculations with non-zero boundary fluxes to simulate inflow and outflow of plasma. There is an upper limit to the upward flux since the upward flow of ions is diffusion limited when there is no external upward electrical driving force (Banks and Kockarts, 1973). For the calculations presented here, we have assumed $T_i = T_e = T$, the neutral temperature. This should be adequate within a few scale heights above the electron density maximum. However, above this region T_e then T_i will increase (Henry and McElroy, 1969; Goertz, 1973; Nagy *et al.*, 1976). Neverthless, our major conclusions should not be affected.

One fairly serious omission from our calculations (and those of others) is the inclusion of the ionization due to the particles that excite the

H_2 Lyman and Werner bands. This is really not too surprising since we still do not know the details of the energy spectrum well enough to make a firm statement regarding ionization. As noted earlier the amount of energy deposited on the dayside appears to be about 0.3 erg cm^{-2} s^{-1}. This is equivalent to about 5×10^9 ion pairs cm^{-2} s^{-1}, somewhat more than created by solar photons. On the basis of preliminary analysis Broadfoot *et al.* (1981) tentatively suggested that the energy may be deposited at H_2 densities $\simeq 10^7$–10^8. Thus 5×10^9 ion pairs cm^{-2} s^{-1} would be created in a region where the ion production by solar photons is much smaller. However, in the discussion we will consider this omission and surmise how it may affect our conclusions.

4. RESULTS

Figure 3(a) shows the electron density profiles obtained for various latitudes, with $k_2 = 0$, day/night averaged ionization rates and $W_D = 0$ for atmospheric model A. The topside plasma is in diffusive equilibrium. The decrease in scale height with increasing latitude reflects the increase of **g** with latitude along a geopotential surface. The lower regions of the plasma are in photochemical steady state (PCSS). The transition height from PCSS to diffusion is given when the chemical time constant for radiative recombination is equal to the diffusion time constant, t_D,

$$t_D = H_p^2/(D_{in} \sin^2 I)$$

where H_p is the plasma scale height. Since I increases with latitude this transition height will decrease with latitude, as we can see in Fig. 3(a). The altitude of the peak electron density remains sensibly constant with latitude. For a simple Chapman layer one would expect the altitude of the peak to increase with latitude. However, the layer is composite and this tends to wash out the increase until near sunset. Also the decrease in the geopotential altitude with latitude tends to lower the height of the peak. This decrease is to first order $\Delta g \cdot z/g$ where z is the altitude above the 1 mb level.

Figure 3(a) also shows the electron density calculated with the same parameters, for the latitude of 40° and using model B. As expected, the peak occurs at lower altitudes since the 10^{11} cm^{-3} [or $\tau(H_2) \simeq 1$] level is lower in this model. The topside plasma scale height is larger reflecting the fact that this model is also warmer than model A at most altitudes (see Fig. 2).

Figure 3(b) shows the results obtained using model A when the upper boundary condition is modified to simulate the inflow or outflow of plasma. For the latitudes used in Fig. 3(a) we have set $\phi_T(H^+) = -2 \times 10^8$ ions cm^{-2} s^{-1}, where $\phi_T(i)$ is the top boundary flux for ion i. This influx may be compared with the diurnally averaged ionization rate of H_2 and H at a latitude of 40°, 6×10^8 ions cm^{-2} s^{-1}, and the H^+ production rate, 1.3×10^8 cm^{-2} s^{-1}. The detailed effect of this inflow of plasma depends on the latitude. For high latitudes where the transition height between diffusion and chemistry is relatively low, the inflow increases the magnitude and raises the height of the peak electron density. For low latitudes where the transition altitude is higher the ion influx cannot readily penetrate this transition region and so a second layer forms above the main photoionization layer. Also shown in Fig. 3(b) for a latitude of 40° are the effects of a somewhat reduced inflow of ions, -10^8 cm^{-2} s^{-1} and an outflow of ions equal to 5×10^7 cm^{-2} s^{-1}. In the latter case, the upward flow lowers the scale height below that expected for a diffusive equilibrium model. An upward flow much larger than 5×10^7 cm^{-2} s^{-1} cannot be sustained because we soon run into diffusion flow for these particular parameters.

Figure 3(a) also shows the photochemical steady state solution (PCSS), i.e. with $(\partial \phi_i/\partial z) = 0$ for a latitude of 40°. From a comparison of this with the flow models it is clear that with this chemistry a PCSS solution is reasonable. However, diffusion does modify the peak densities somewhat but the electron density peak is essentially recombination limited, i.e. an $F1$ region.

The results in Fig. 4 were obtained by using a diurnal sun running the program until cyclic conditions were obtained. The computations were run for a latitude of 40°, $I = 59.2°$ and for 3 non-zero values of k_2, 10^{-15}, 10^{-14} and 10^{-10} molecule^{-1} cm^3 s^{-1}. For $k_2 = 10^{-15}$ and 10^{-14} the conversion of protons to H_2^+ and H_3^+ is rapid and the electron densities are accordingly reduced. Also the identity of the main ion is modified. For $k_2 = 0$ the main ion is H^+ at all heights, while for $k_2 = 10^{-15}$ and 10^{-14} the main ion in the lower region is H_3^+. The minimum possible electron densities are obtained with $k_2 = 10^{-10}$, since with k_2 this large, each proton is rapidly converted to H_3^+ and radiative recombination of H^+ does not play an important role. Also flow is unimportant and, aside from temperature effects on k_7, the shape of the electron density profile reflects the ionization rate.

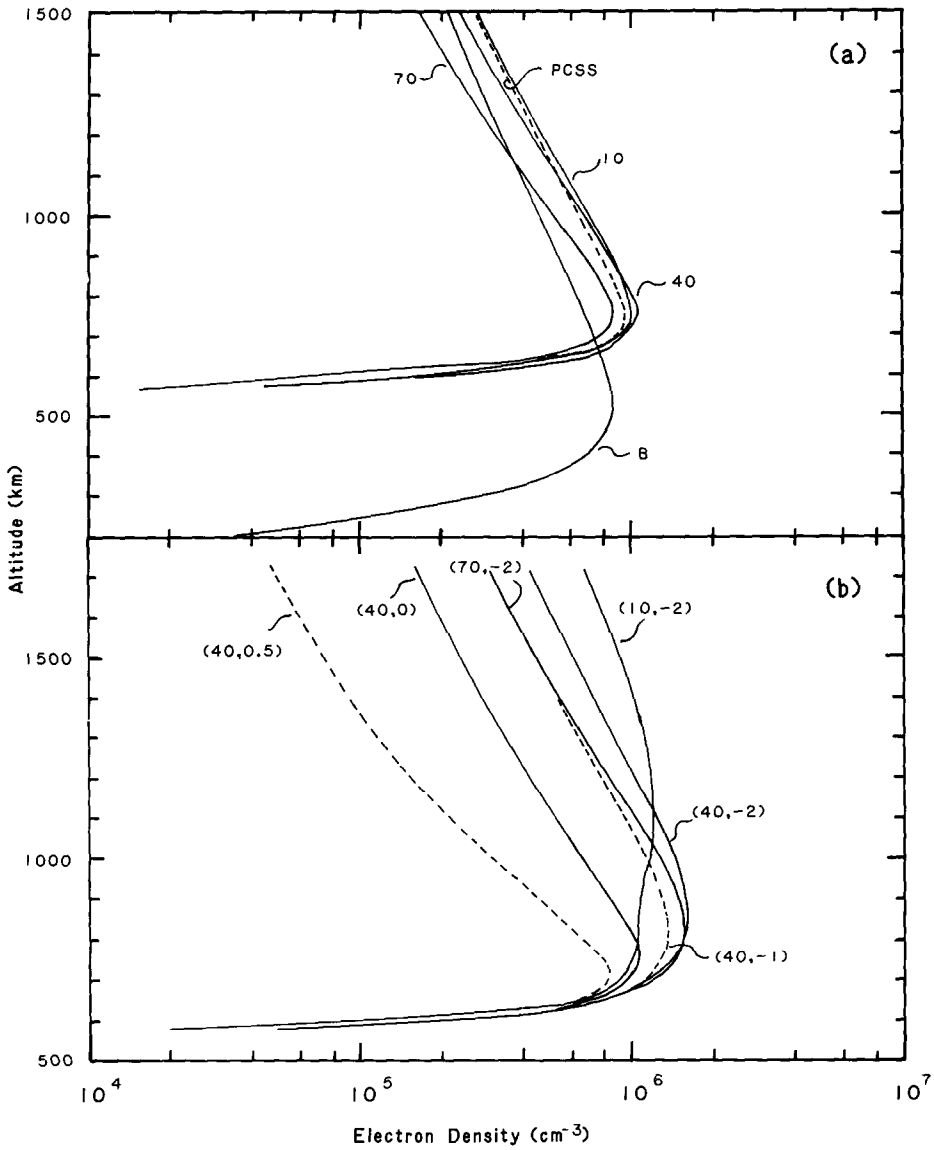

FIG. 3(a). MODEL ELECTRON DENSITY PROFILES CALCULATED USING THE ATMOSPHERES A OF FIG. 2 FOR 3 LATITUDES 10°, 40° AND 70°.
The curve marked PCSS was calculated using photochemical steady state. The curve marked B was calculated using the model atmosphere B of Fig. 2 for a latitude of 40°. For all the calculations $W_D = 0$, $\phi_T(H^+) = 0$ and $k_2 = 0$. Ionization rates were diurnally averaged.

FIG. 3(b). ELECTRON DENSITY PROFILES USING MODEL ATMOSPHERE A.
The curves are labelled (X, Y) where X gives the latitude and Y gives the outflux of protons in units of 10^8 cm^{-2} s^{-1}. $W_D = 0$, $k_2 = 0$.

Figure 4 gives the electron density profiles for noon, and solar zenith angles of 90° (sunrise and sunset). In contrast to the results with $k_2 = 0$, the electron density below the peak decreases as the sun sets and continues to decrease dramatically during the night, while ions from above the peak flow down to the $H^+ + H_2$ sink. For the values of k_2 of 10^{-15} and 10^{-14} the peak is defined by diffusion vs recombination, i.e. above the peak the ions are in diffusive equilibrium, while below

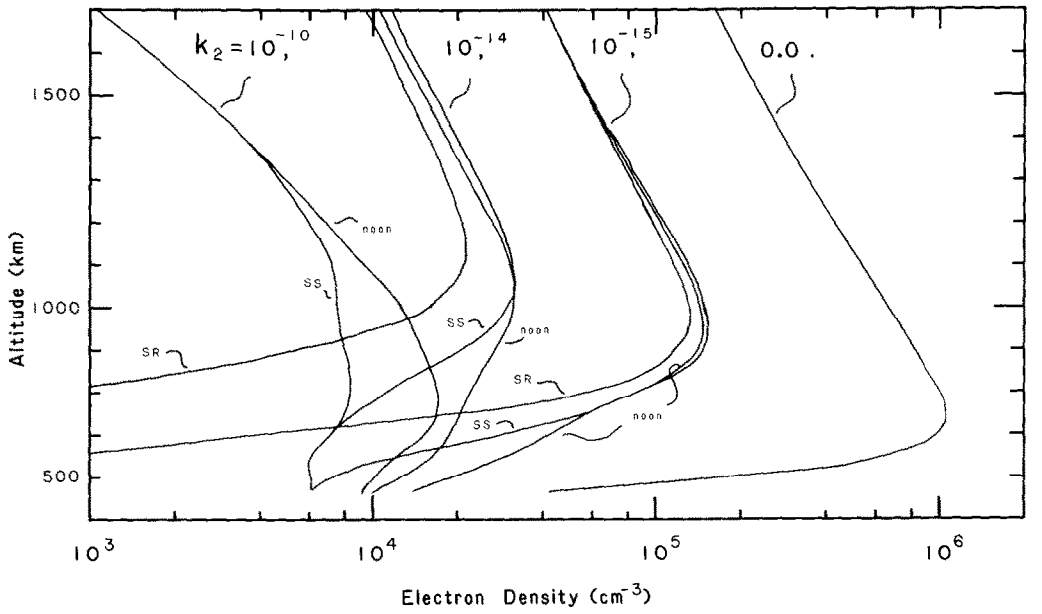

FIG. 4. ELECTRON DENSITY PROFILES CALCULATED FOR ATMOSPHERE A, AND DIURNAL IONIZATION RATES FOR A LATITUDE OF 40°.
The curves are labelled by the values of k_2 used. SR and SS apply to sunrise and senset respectively.

the peak the ions are in chemical equilibrium. Thus for this type of model the ionospheric peak is an $F2$-type peak, rather similar to the earth's. The altitude of the peak electron density increases as k_2 is increased. This is as a result of the peak being formed by competition between diffusion and chemistry. As k_2 is increased, the chemical time constant decreases. For a peak to form the diffusion time constant must decrease. This is effected by the peak forming at higher altitudes. The main difference between this type of $F2$ region and the terrestrial type is that, even with $k_2 = 10^{-14}$ or 10^{-15}, chemical loss times are still so much slower on Jupiter that the nighttime decay of the peak is less than a factor of two, much less than is the case for the earth when no vertical drifts occur.

The calculations shown thus far have been for k_2 constant with altitude. It is unlikely that this is the case. Thus we have done some calculations with a height dependent rate, which we estimate as follows. We assume that the A factor for the rate is given by the gas kinetic rate, while we assume an activation energy based on the endothermicity of the reaction. The rate adopted was

$$k_2 = 2 \times 10^{-9} \exp(-21240/T_v)$$

where T_v is the vibrational temperature. For simplicity we have calculated electron densities with $T_v = 2T$ and $T_v = 3T$. These calculations are shown in Fig. 5 along with electron densities with $k_2 = 0$ and $k_2 = 10^{-15}$. They are all for average insolation conditions. Note that compared with the results for a k_2 that is independent of altitude, the peak remains low and the density stays relatively high. This is, of course, due to the low T giving small values for k_2 in the lower regions of the ionosphere. As we will see in the next few paragraphs, this situation may be modified by vertical drifts. These calculations indicate that one must be careful in generalizing too much from this type of exploratory calculation.

The calculations shown in Fig. 3–5 were made with $W_D = 0$. On the earth the component of the meridional wind parallel to the magnetic field can raise or lower the $F2$ peak by blowing plasma up or down the field lines, or it can prevent the decay of the $F2$ layer by maintaining the peak at higher altitudes where chemical loss times are longer (e.g. Strobel and McElroy, 1970; Banks and Kockarts, 1973). However, in the Jovian ionospheric models the effect of small meridional winds is much more pronounced since the recombination time constant is so long. Thus in Fig. 6 we show the effect of vertical drifts of $+15\ m\ s^{-1}$, $+5\ m\ s^{-1}$, and $-5\ m\ s^{-1}$. As noted above, the effect of small plasma drifts are substantial due to the long time

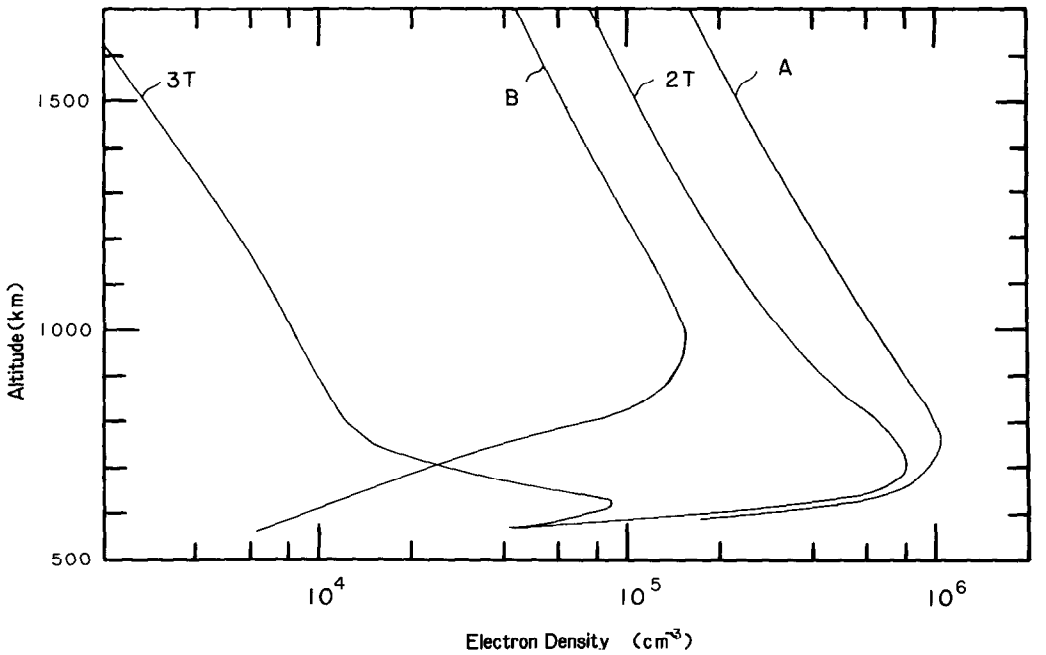

FIG. 5. ELECTRON DENSITY PROFILES FOR AVERAGE INSOLATION CONDITIONS AND VARIOUS VALUES OF k_2 AT A LATITUDE OF 40°.

Curves A and B are for $k_2 = 0$ and 10^{-15} cm^3 s^{-1} respectively. The curves labelled $2T$ and $3T$ use these values of temperature for T_v and the rate expression given in the text. $\phi_T(H^+) = 0$, $W_D = 0$.

constants involved. For an upward drift of 15 m s^{-1}, the peak electron density is formed at the location where the diffusion time constant is equal to the flow time constant $t_f = H_p/W_D$. Above this altitude diffusive equilibrium is a good approximation (unless $\phi_T \neq 0$) while below the drift effect prevails. The peak electron density remains at about the same value of 1.0×10^{-6} even though the H^+ recombination rate, k_5, in the region of the peak density is decreased. However the width of the peak increases to compensate. For $W_D =$ 5 m s^{-1} the time constants are sufficiently long that recombination plays a role in the location of the electron density peak. The peak forms where the flow time constant is balanced by the diffusion down and recombination. The change of the peak density with change in plasma drift velocity is much smaller than is the case for the earth since the radiative recombination loss reaction rate does not depend strongly on altitude.

With downward drift velocities the H^+ ions are pushed down to the region of higher H_2 densities where H^+ forms H_3^+ via reaction k_1 and this then recombines via reaction k_7, i.e.

$$H^+ + H_2 + M \rightarrow H_3^+ + M$$
$$H_3^+ + e \rightarrow H_2 + H$$
$$\rightarrow 3H.$$

The peak forms in the region where t_f is comparable to the time constant for the loss of H^+. As the downward drift speed increases the peak is pushed further and further down. In Fig. 6 we show the results for $W_D = -5$ m s^{-1}. For this case we used a velocity boundary condition for the lower boundary with the imposed velocity equal to the flow velocity. We should note that with this boundary condition about 2/3 of the ions produced flow out the bottom of our model to be recombined at higher H_2 densities.

Figure 6 also shows the effect of combining vertical drift with vibrational excitation of H_2. Comparing the results in Figs. 5 and 6, both with $T_v = 2T$ but for $W_D = 0$ and 5 m s^{-1}, we see that the peak electron density is moved to greater heights by the drift, in this case from 700 to 1100 km. Also, although the peak density has decreased by a factor of two, the plasma densities

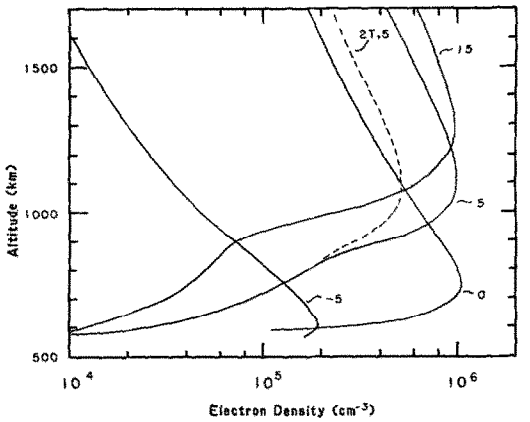

FIG. 6. ELECTRON DENSITY PROFILES CALCULATED FOR VARIOUS VALUES OF W_D FOR A LATITUDE OF 40°. The curves are labelled (X) where X is a value of the drift velocity in m s^{-1}. $\phi_T(H^+) = 0$. The curves for X = 5 and 15 were calculated with a lower boundary condition of zero input flux. The curve marked −5 is for a velocity boundary condition; the velocity was set equal to W_D at the lower boundary. The dashed curve is for W_D = 5 m s^{-1} and $T_n = 2T$.

above the peak are enhanced over the case without flow due to the flux from below.

For the calculations with non-zero W_D we have found that the finite difference approximation to the differential equations was not sufficiently accurate, at the step sizes we could readily use, to accurately estimate the effect of a slow chemical loss vs very fast wind and diffusion times. Convergence was obtained but the densities were inaccurate. Thus we imposed the condition for solution that the integrated net production for each ion in the model should equal the net outflow through the boundaries. At the upper boundary this outflow was calculated by estimating the net chemical loss in the region beyond the boundaries. In effect wind and diffusion are allowed to distribute the ions while the integrated condition ensures conservation of ions.

5. DISCUSSION

In Fig. 1 we have sketched in the standard ionospheric models (i.e. with $k_2 = 0$, $W_D = 0$ and model atmosphere A). For *Pioneer* the H densities were reduced by a factor of 100 making H_2 the principal source of H^+. Solar fluxes were reduced by a factor of 3 to simulate *Pioneer* conditions. Bearing in mind that the thermosphere may have been cooler at the time of *Pioneer* encounter, i.e. the ionosphere peak would be lower, we see that the calculated ionospheric peak is well below any of the principal layers. Also the density of the peak is greater. From Fig. 3(a) it can be seen that the effect of latitude on the model peak altitude is trivial, while from Fig. 3(b) it is apparent that inflow or outflow of plasma has a small effect on modifying the peak altitude except for small dip angles. Using the data from Fig. 4 as a guide one could obtain reasonable agreement in the altitude of the L_3 peak and possibly its density also if k_2 were somewhat less than 10^{-15}. However, how does one account for the L_1 peak?

Likewise, Fig. 1(b) contains the standard electron density profile appropriate for *Voyager* conditions. In this case H and H_2 are both important sources of H^+, the relative importance depending on altitude. We note that as for *Pioneer*, neither the magnitude nor the location of the peak in the model electron density match the observations.

In order to see the error involved in deducing model atmospheres from the electron density profiles, we have followed the procedure of Atreya and Donahue (1976, 1979b) and adjusted the model atmosphere parameters to obtain a fit. The atmosphere chosen is shown in Fig. 2. It was not optimized in any fashion. The column amount of H used was constrained by the Lyman α albedo to be $\leqslant 3 \times 10^{17}$ cm^{-2}. In any case, production of H^+ from H is an important but not the major source of H^+ at the model ionospheric peak. The altitude of the electron density peak calculated from this model atmosphere is about 1750 km, intermediate between that of V1 entrance and V2 exit profiles. The magnitude of the peak electron density is more than a factor of two too large. To reduce the peak density we set $k_2 = 2 \times 10^{-16}$. With this value of k_2 there is no large day to night variation in the peak electron density calculated. Specifically the model with $k_2 = 2 \times 10^{-16}$ does not reduce to the exit curve for V1 as was suggested by Atreya *et al.* (1979b) and Strobel (1979).

From Fig. 2 we see that using the model atmosphere obtained by fitting the electron density profiles gives $\tau(H_2)$ at 700 Å $\gg 1$ over a much larger altitude range than that obtained from the UVS occultation data. In fact $\tau = 1$ occurs approximately at 3200 km, i.e. about 1700 km above where we deduce $\tau = 1$ from the occultation data. Given the information available from the UVS data such an uncertainty is inconceivable. Thus we cannot adjust the model atmosphere in any substantial way to obtain agreement with the electron density profiles. The question is then whether we can obtain agreement using the UVS model atmospheres and by adjusting k_2 and W_D.

We first try to fit the V1 electron density profiles, and use model atmosphere A. Necessary parameters such as dip angle are given in Table 1. The variation of gravity with latitude was calculated using the formulae of Anderson (1976). The calculated curves are shown for entrance and exit measurements in Fig. 1(b). With $W_D = 25\ m\ s^{-1}$ and $k_2 = 9 \times 10^{-15}\ cm^3\ s^{-1}$ we obtain reasonable agreement with the V1 entrance data. If this value of k_2 is correct it implies substantial vibrational excitation. The thermal rate for $H^+ + H_2$ elastic collisions is $\sim 2 \times 10^{-9}\ cm^3\ s^{-1}$ (cf. Huntress, 1974). Thus if every collision of H^+ with H_2 in the $v \geq 4$ level resulted in reaction a value of $k_2 = 9 \times 10^{-15}$ would imply that a fraction, $F = 5 \times 10^{-6}$, of H_2 molecules would be in vibrational levels ≥ 4. Figure 7 gives this fraction, F, vs vibrational temperature. Thus for $k_2 = 9 \times 10^{-15}$ this would imply an H_2 vibrational temperature of 1750 K. However, this temperature may be too low, since the efficiency of the reaction may not be unity. As we noted for 8 eV photons the efficiency is $< 10\%$. Thus, if this situation obtains for vibrationally excited H_2, then the vibrational temperature deduced from k_2 would be even higher. Also, k_2 has been taken as independent of altitude. Thus much recombination takes place at lower altitudes. If k_2 took the Arrhenius form given earlier then many of the ions would not recombine near the source and would flow to the peak. So again k_2 or T_v would have to be increased to obtain a fit.

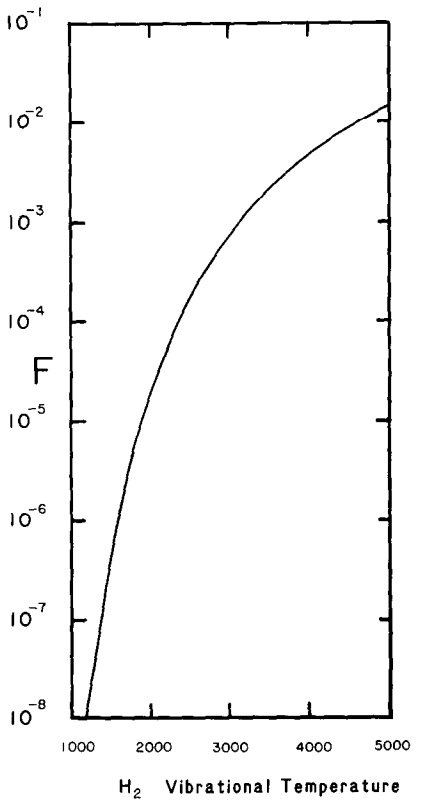

FIG. 7. FRACTION, F, OF H_2 IN THE VIBRATIONAL LEVELS $v \geq 4$ VS VIBRATIONAL TEMPERATURE FOR H_2 IN VIBRATIONAL EQUILIBRIUM.

Using the above parameters the calculated topside scale height is larger than that of the V1 entrance profile. Thus the difference between the observed and calculated scale heights might suggest that perhaps our temperatures are too high by about a factor of two. This possibility seems unlikely since the UVS solar occulation data and the Radio Science data were obtained in relative proximity. An alternative possibility for reducing the scale height could be outward flow, but the flow of ions inferred, $\sim 10^9\ cm^{-2}\ s^{-1}$, is much greater than the total production of H^+ in the model. However we note that it is of the order of the ion production rate deduced from airglow data that we commented on earlier.

Even with $k_2 = 9 \times 10^{-15}\ cm^3\ s^{-1}$ there is no substantial day to night decay since the peak is located at altitudes where H_2 densities are low and so H^+ loss time constants are long. Thus fitting the V1 entrance measurements does not fit the exit measurements. Fitting the V1 exit measurements requires even larger values of k_2 and W_D to obtain reasonable agreement with the measurements. The profile obtained with $k_2 = 5.5 \times 10^{-13}\ cm^3\ s^{-1}$ and $W_D = 40\ m\ s^{-1}$ is shown in Fig. 1(b). The peak is located in the correct region for V1 exit and the electron density peak is reasonable. The value of k_2 obtained implies a minimum value for T_v of 2700 K. The peak is so far away from the source region that the wind of $40\ m\ s^{-1}$ is required to be effective for a full Jovian day. If the wind direction changes with time of day, as is the case on the earth, then even stronger winds are required to maintain a peak at this altitude.

In attempting to fit the V2 measurements we again require different conditions for entrance and exit. Both model curves are shown in Fig. 1(b). For exit $k_2 = 1.2 \times 10^{-13}$ and $W_D = 400\ m\ s^{-1}$ gives correct peak densities and a peak located at the correct altitude. The implied T_v is > 2000 K. The wind of $400\ m\ s^{-1}$ required to maintain the peak is quite substantial! It might seem strange that while a $25\ m\ s^{-1}$ wind can maintain the V1 entrance peak a 14 times faster wind is required to maintain a peak only some 350 km or one H scale height

higher. However the density difference is about a factor of 13. At the V1 peak the background density is 75% H_2 while at the V2 peak it is 60% H. The density difference is a reflection of the transition from H_2 to H and also of the smaller scale heights at higher latitudes due to a value of g that is 10% larger. The effect of smaller scale heights is of course amplified by the large vertical extent of the ionosphere. The changes in the effective diffusion coefficient at the peak for the V1 and V2 cases due to different major species and different dip angles largely cancel each other.

It is clear that the W_D of 400 m s^{-1}, (if this is in fact what is causing the peak) cannot be caused by a neutral wind. From Table 1 we see that the dip angle is 85.5°. If W_D were caused by neutral winds only, then $V_n = -W_D/[\sin(I)\cos(I)] = -5.1$ km s^{-1}! It seems more likely that the drift velocity may be caused by electric fields.

In fitting the V2 exit data we have assumed a neutral atmosphere temperature and structure similar to that used for lower latitudes. If the high latitude thermosphere were warmer, then higher densities would obtain at the same altitudes, diffusion coefficients would be smaller, and so slower winds would be required to form the peak.

For the exit measurements we find that with $k_2 = 0.0$ and a drift velocity of $W_D = -4$ m s^{-1} we obtain reasonable agreement with the V2 exit profile below 1000 km. From Fig. 4 we estimate that a value of $k_2 > 10^{-15}$ cm^3 s^{-1} in combination with downward flow would produce electron densities that are too small. With the model parameters used to fit the V2 exit measurements information is obtained only for the region between 500 and 1000 km or densities from 10^{10} to 10^{12} cm^{-3}. Thus, using the above limit to k_2, it seems that the vibrational temperature of H_2 is probably < 1500 K at these densities. Thus there appears to be no pronounced auroral signature in the electron density profile in this altitude region. This probably just reflects the efficiency of H_2 vibrational quenching by H_2 and H (Audibert *et al.*, 1974; Heidner and Kasper, 1972). For the $v = 1$ vibrational level of H_2 the quenching time constant is ~ 1000 s at 700 km and 100 s at 500 km for model A. Above 1000 km the measured scale height is larger than that calculated by the model. This may reflect the fact that $T_e > T_i > T$ above 1000 km. Elevated electron temperatures would suggest input of energy either by hot thermalised plasma or by non-thermal precipitation.

The altitude regime that the model parameters are sensitive to when fitting the V2 entrance data is 500–1000 km. This is in contrast to the *other Voyager* RSS measurements, where information is only available above 1500 km or so, i.e. a density level $\leqslant 10^8$ cm^{-3}. At these density levels vibrational quenching is mainly due to H (for Voyager conditions). But the time constant $\geqslant 10^5$ s is so long that vibrational energy is lost mainly by diffusion. The vibrational–vibrational energy transfer mechanism has a time constant $\geqslant 10^4$ s for the lower H_2 vibrational levels. Thus we can expect that the vibrational temperature of the ground state of H_2 is not equilibrated with the kinetic temperature, and that the k_2 rates that we have been suggesting may not be unreasonable. In fact, what seems more likely at these altitudes is that the values of k_2 used refer to an average over a non-thermal vibrational distribution and not to a vibrational distribution in thermal equilibrium. This suggests that the values of T_v used should only be taken as indicators of the degree of disequilibrium present in the exosphere.

We have mentioned earlier that there is a possibility of a large ion production rate $\sim 5 \times 10^9$ cm^{-2} s^{-1} on the dayside. What effect might this have on our results? Obviously the nature of the effect will be a function of the altitude where the ions are created. If they are created below 1000 km say, and a vertical drift is present then k_2 and T_v will have to be even higher than we have estimated in order to obtain agreement with the measurements. Also the wind will tend to smooth any structure caused by the precipitation. If the ions are produced at the 10^7–10^8 density level what are the consequences? First the main ion produced would probably be H^+. We estimate that the H_2^+ produced would recombine locally and add, at most, 10^4 ions cm^{-3} to the ionosphere. Second, the vibrational temperature necessary to supress the H^+ density to 2×10^5 cm^{-3} is > 3000 K with $k_2 = 1.7 \times 10^{-12}$ cm^3 s^{-1}. Even with k_2 this fast, chemical lifetimes are much longer than diffusion lifetimes in the region of the V1 and V2 L_1 peaks. Thus the H^+ will flow away from the ionization source and the location of the peak is still determined by a balance between diffusion and the ion wind. One consequence, briefly alluded to earlier, is that an upper atmospheric ion source could provide the ionization for the upward flux suggested by our analysis of the V1 entrance data.

We caution that the details of these fits to the radio science electron density profiles should not be taken too seriously. As we noted earlier, with winds of the magnitude that we have used, the peaks are formed by competition between down-

ward diffusion and upward flow. At the peak levels the recombination times are still quite long, several days. Thus it is unlikely that the plasma is even in a steady state at these altitudes due to the temporal behaviour of neutral winds and electric fields.

We have not attempted a detailed analysis of the *Pioneer* profiles. It might appear that the occurrence of the L_1 peak in the same region as the Voyager profiles, might suggest vibrationally enhanced H_2 and substantially vertical drift velocities. This type of explanation, however, will not account for the simultaneous occurrence of the L_1 and L_3 peaks as may be seen from Fig. 1(b), 5 and 6. As we can see from these figures, producing a peak in the 1500–2000 km region washes out the structure in the region below and no L_3 type feature can appear. Thus it becomes imperative to know if the L_3 peaks and those lower are in fact real or artifacts of the data analysis. In addition analysis of the V1 and V2 data below the peaks would add valuable information in our attempts to understand the ionospheric profiles. If the layering is real it is possible that it is caused by electric field effects, wind shears, or the presence of metallic ions such as Na^+ (see e.g. Atreya and Donahue, 1976).

From the measurements and our attempts to fit them, it seems clear that the changes in the ionospheric profiles from entrance to exit are not simply related to solar insolation changes, i.e. sunset vs sunrise. The differences may be due to different thermospheric winds and probably differing precipitation patterns. For example, the entrance radio science occultation experiment for V1 is in the region of the H bulge. It is likely that the localized H bulge (Sandel *et al.*, 1980) marks a region of harder particles convected in from the magnetosphere (Dessler *et al.*, 1981) while the planet-wide H_2 band emission is excited high in the atmosphere by softer particles (Broadfoot *et al.*, 1981). This softer flux in the V1 exit region would give rise to higher vibrational temperatures. This is certainly consistent with our analysis of the electron density profiles.

In our calculations we have not allowed for the production of ions by precipitating particles. From the discussion it should be clear that even without this effect the model can provide the needed ionization. Thus any allowance for precipitation would tend to imply larger values for k_2 and so even larger vibrational temperatures for H_2. As we have already indicated precipitation will not affect the mode of formation of the high altitude peak, i.e. balance between upward ion winds and downward diffusion.

Most of our calculations have been for k_2 constant with altitude. It seems unlikely that this is the case and in further work we will attempt to calculate vibrational temperatures of H_2 in the thermosphere and see how this may modify our results.

Finally the situation we have outlined here for Jupiter may also apply to Saturn. A preliminary comparison of the solar occultation observed by the V1 UVS at Saturn with the radio science (Tyler *et al.*, 1981) ionosphere results show a similar situation regarding the extent and location of the ionosphere relative to the neutral atmosphere.

6. CONCLUSIONS

We have used the neutral model atmospheres derived from the UVS solar and stellar occultation data to calculate electron density profiles. Using pre-*Voyager* concepts of photochemical steady state models we have shown that this simple type of model is not adequate to explain the observed electron density profiles. Meridional winds (or electric fields) have the effect of moving the plasma through large vertical distances due to the long recombination time constants involved and can account for the observed electron density profiles. We have also shown that the electron densities calculated using standard parameters are much larger than those measured by the *Pioneer* and *Voyager* radio science experiments. To reduce the electron densities we have adopted an idea originally proposed by McElroy (1973) who suggested that vibrational excitation of H_2 may be important. However to obtain fits to the RSS electron density data we find that there is no single vibrational temperature appropriate to the whole thermosphere. One must invoke vibrational temperatures and vertical upward and downward drifts which vary with geographical and/or magnetic location in order to produce reasonable fits to the ionospheric profiles. In addition it appears as if outflow (and possibly inflow) of plasma may play a role in defining the electron density profiles.

The profiles measured by *Pioneer* 10 and 11 seem even more difficult to understand in terms of uniform conditions. In fact, if we use the models applied to the *Voyager* data we cannot simultaneously obtain L_1 and L_3 peaks. One explanation is that the L_3 peak is an artifact of the data analysis. Another is that our model is not adequate. Perhaps electric fields play some role in

deforming the electron density profiles from those calculated by our simple models. What is clear however is that the ionospheric profiles do not directly yield information on the neutral atmosphere. They reflect more the action of the neutral atmosphere on the ionosphere via winds and the interaction of the magnetosphere with the neutral atmosphere via particle precipitation.

Acknowledgements—This work was supported by the JPL, California Institute of Technology, under NASA contract NAS 7-100. Additional support was provided by the Planetary Sciences Discipline in NASA's Office of Space Sciences.

REFERENCES

Anderson, J. D. (1976). The gravity field of Jupiter, in *Jupiter* (Ed. Gehrels, T.), pp. 113–121, Univ. Arizona Press, Tucson.

Atreya, S. K. and Donahue, T. M. (1976). Model ionospheres of Jupiter, in *Jupiter* (Ed. Gehrels, T.), pp. 304–318, Univ. Arizona Press, Tucson.

Atreya, S. K., Donahue, T. M., Sandel, B. R., Broadfoot, A. L. and Smith, G. R. (1979a). Jovian upper atmospheric temperature measurements by the Voyager 1 UV spectrometer. *Geophys. Res. Letts.* 6, 795–798.

Atreya, S. K., Donahue, T. M. and Waite, J. H. Jr. (1979b). An interpretation of the Voyager measurement of Jovian electron density profiles. *Nature, Lond.* **286**, 795–796.

Audibert, M. M., Coffrin, C. and Ducuing, J. (1974). Vibrational relaxation of H_2 in the range 500–40 K. *Chem. phys. Lett.* **25**, 158–163.

Auerbach, D., Cacak, R., Caudano, R., Gaily, T. D., Keyser, C. J., McGowan, J. W., Mitchell, J. B. A. and Wilk, S. F. J. (1979). Merged electron–ion beam experiments I. Methods and measurements of $(e–H_2^+)$ and $(e–H_3^+)$ dissociative–recombination cross sections. *J. Phys. B.* **10**, 3797–3820.

Banks, P. M. and Kockarts, G. (1970). *Aeronomy* Vols. A and B, Academic Press, New York.

Bardsley, J. M. and Biondi, M. A. (1970). Dissociative recombination, in *Ad. Atom. Mol. Phys.*, Vol. 6 (Ed. Bates, D. R. and Estermann, I.), pp. 1–57, Academic Press, New York.

Bates, D. R. and Dalgarno, A. (1962). Electronic recombination, in *Atomic and Molecular Process* (Ed. Bates, D. R.), pp. 245–271, Academic Press, New York.

Broadfoot, A. L., Belton, M. J. S., Takacs, P. Z., Sandel, B. R., Shemansky, D. E., Holberg, J. B., Ajello, J. M., Atreya, S. K., Donahue, T. M. Moos, H. W., Bertaux, J. L., Blamont, J. E., Strobel, D. F., McConnell, J. C., Dalgarno, A., Goody, R. and McElroy, M. B. (1979). Extreme ultraviolet observations from Voyager 1 encounter with Jupiter. *Science N.Y.* **204**, 979–982.

Broadfoot, A. L., Sandel, B. R., Shemansky, D. E., McConnell, J. C., Smith, G. R., Holberg, J. B., Atreya, S. K., Donahue, T. M., Strobel, D. F. and Bertaux, J. L. (1981). Overview of the Voyager ultraviolet spectrometry results through Jupiter encounter. *J. geophys. Res.* **86**, 8259–8284.

Browning, R. and Fryar, J. (1973). Dissociative photoionization of H_2 and D_2 through the $1s\sigma_g$ ionic state. *J. Phys. B* **6**, 364–371.

Carlson, R. W. and Judge, D. L. (1974). Pioneer 10 ultraviolet photometer observations at Jupiter encounter. *J. geophys. Res.* **79**, 3623–3633.

Cochran, W. D. and Barker, E. S. (1979). Variability of Lyman-alpha emission from Jupiter. *Astrophys. J.* **234**, L151–154.

Dalgarno, A. and Allison, A. C. (1969). Photodissociation of molecular hydrogen on Venus. *J. geophys. Res.* **74**, 4178–4180.

Dessler, A. J., Sandel, B. R. and Atreya, S. K. (1981). The Jovian hydrogen bulge: evidence for co-rotating magnetospheric convection. *Planet. Space Sci.* **29**, 215–224.

Eshleman, V. R., Tyler, G. L., Wood, G. E., Lindal, G. F., Anderson, J. D., Levy, G. S. and Croft, T. A. (1979a). Radio science with Voyager 1 at Jupiter: Preliminary profiles of the atmosphere and ionosphere. *Science, N.Y.* **204**, 976–978.

Eshleman, V. R., Tyler, G. L., Wood, G. E., Lindal, G. F., Anderson, J. D., Levy, G. S. and Croft, T. A. (1979b). Radio science with Voyager at Jupiter: Initial Voyager 2 results and a Voyager 1 measure of the Io torus. *Science, N.Y.* **206**, 959–962.

Festou, M. C., Atreya, S. K., Donahue, T. M., Sandel, B. R., Shemansky, D. E. and Broadfoot, A. L. (1981). Composition and thermal profiles of the Jovian upper atmosphere determined by the Voyager ultraviolet stellar occultation experiment. *J. geophys. Res.* **86**, 5715–5725.

Fjeldbo, F., Kliore, A., Seidel, B., Sweetnam, D. and Woiceshyn, P. (1976). The Pioneer 11 radio occultation measurements of the Jovian ionosphere, in *Jupiter* (Ed. Gehrels, T.), pp. 238–246, Univ. Arizona Press, Tucson.

Fjeldbo, G., Kliore, A., Seidel, B., Sweetnam, D. and Cain, D. (1975). The Pioneer 10 radio occultation measurements of the ionosphere of Jupiter. *Astron. Astrophys.* **39**, 91–96.

Fryar, J. and Browing, R. (1973). Molecular photoionization at 584Å and 304Å. *Planet. Space Sci.* **21**, 709–711, Erratum, *Ibid.* **21**, 1080.

Goertz, C. K. (1973). Jupiter's ionosphere and magnetosphere. *Planet. Space Sci.* **21**, 1389–1398.

Heidner, R. F. III. and Kasper, J. V. V. (1972). An experimental rate constant for $H + H_2(v = 1) \rightarrow H + H_2(v = 0)$. *Chem. phys. Lett.* **15**, 179–184.

Henry, R. J. W. and McElroy, M. B. (1969). The absorption of extreme ultraviolet solar radiation by Jupiter's upper atmosphere. *J. Atmos. Sci.* **26**, 912–917.

Hudson, R. D. (1971). Critical review of ultraviolet photoabsorption cross-sections for molecules of astrophysical and aeronomic interest. *Rev. Geophys. Space Phys.* **9**, 305–406.

Hunten, D. M. (1969). The upper atmosphere of Jupiter. *J. Atmos. Sci.* **26**, 826–834.

Hunten, D. M. and Dessler, A. J. (1977). Soft electrons as a possible heat source for Jupiter's thermosphere. *Planet. Space Sci.* **25**, 817–821.

Hunten, D. M. and Veverka, J. (1976). Stellar and spacecraft occultations by Jupiter: a critical review of derived temperature profiles, in *Jupiter* (Ed. Gehrels, T.), pp. 247–283, Univ. of Arizona Press, Tucson.

Huntress, W. T. (1974). A review of Jovian ionospheric chemistry, in *Ad. Atomic Mol. Phys.* Vol. 10 (Ed. Bates, D. R. and Estermann, I.), pp. 295–340, Academic Press, New York.

Judge, D. L., Carlson, R. W., Wu, F. M. and Hartmann,

U. G. (1976). Pioneer 10 and 11 ultraviolet photometer observations of the Jovian satellites, in *Jupiter* (Ed. Gehrels, T.), pp. 1068–1101, Univ. Arizona Press, Tucson.

Lee, L. C., Carlson, R. W. and Judge, D. L. (1976). The absorption cross-sections of H_2 and D_2 from 180 to 780 Å. *J. quant. Spectrosc. Rad. Trans.* **16**, 873–877.

Leu, M. T., Biondi, M. A. and Johnsen, R. (1973). Measurements of recombination of electrons with H_3^+ and H_5^+. *Phys. Rev.* **A8**, 413–419.

McConnell, J. C., Sandel, B. R. and Broadfoot, A. L. (1980a). Voyager UV spectrometer observations of He 584Å dayglow at Jupiter. *Planet. Space Sci.* **29**, 283–292.

McConnell, J. C., Sandel, B. R. and Broadfoot, A. L. (1980b). Airglow from Jupiter's night side and crescent: Ultraviolet spectrometer observations from Voyager 2. *Icarus* **43**, 128–142.

McElroy, M. B. (1973). The ionospheres of the major planets. *Space Sci. Rev.* **14**, 460–473.

Monahan, K. M., Huntress, W. T. Jr., Lane, A. L., Ajello, J. M., Burke, T. E., LeBreton, P. and Williamson, A. (1974). Cross-section for the dissociative photoionization of hydrogen by 584Å radiation: the formation of protons in the Jovian ionosphere. *Planet. Space Sci.* **22**, 143–149.

Nagy, A. F., Chamcides, W. L., Cheu, R. H. and Atreya, S. K. (1976). Electron temperatures in the Jovian ionosphere. *J. geophys. Res.* **81**, 5567–5569.

Prasad, S. S. and Capone, L. A. (1971). The Jovian ionosphere: Composition and temperatures. *Icarus* **15**, 45–55.

Samson. J. A. R. (1966). The measurement of photoionization cross-sections of the atomic gases. *Ad. Atom. Mol. Phys.*, Vol. 2 (Ed. Bates, D. R. and Estermann, I.), pp. 178–261, Academic Press, New York.

Samson, J. A. R. (1972). Observation of double electron excitation in H_2 by photoelectron spectroscopy. *Chem. phys. Lett.* **12**, 625–627.

Sandel, B. R., Shemansky, D. E., Broadfoot, A. L., Bertaux, J. L., Blamont, J. E., Belton, M. J. S., Ajello, J. M., Holberg, J. B., Atreya, S. K., Donahue, T. M., Moos, H. W., Strobel, D. F., McConnell, J. C., Dalgarno, A., Goody, R., McElroy, M. B. and Takacs, P. Z. (1979). Extreme ultraviolet observations from Voyager 2 encounter with Jupiter. *Science*, N.Y. **206**. 962–966.

Sandel, B. R., Broadfoot, A. L. and Strobel, D. F. (1980). Discovery of a longitudinal asymmetry in the H Lyman-alpha brightness of Jupiter. *Geophy. Res. Lett.* 7, 5–8.

Shemansky, D. E. (1980). Radiative cooling efficiencies and predicted spectra of species of the Io plasma torus. *Astrophys. J.* **236**, 1043–1054.

Strobel, D. F. (1979). The ionospheres of the major planets. *Rev. Geophys. Space Phys.* **17**, 1913–1922.

Strobel, D. F. and McElroy, M. B. (1970). The *F*2-Layer at middle latitudes. *Planet. Space Sci.* **18**, 1181–1202.

Strobel, D. F. and Atreya, S. K. (1981). Ionosphere, in *Physics of the Jovian magnetosphere* (Ed. Dessler, A. J.), (to be published).

Tanka, T. and Hirao, K. (1973). Structure and time variations of the Jovian ionosphere. *Planet. Space Sci.* **21**, 751–762.

Thorne, R. T. and Tsurutani, B. T. (1979a). Diffuse Jovian aurora influenced by plasma injection from Io. *Geophys. Res. Lett.* **6**, 649–652.

Tyler, G. L., Eshleman, V. R., Anderson, J. D., Levy, G. S., Lindal, G. F., Wood, G. E. and Croft, T. A. (1981). Radio science investigations of the Saturn system with Voyager 1: Preliminary results. *Science, N.Y.* **212**, 201–205.

Yung, Y. L. and Strobel, D. F. (1980). Hydrogen photochemistry and Lyman-alpha albedo of Jupiter. *Astrophys. J.* **239**, 395–402.